Electronic materials

Facile preparation of aluminum nitride decorated multi-walled carbon nanotube for excellent microwave absorption

Wei Ma[1,2,3], Rui Yang[1,2,3], Hai Xie[1,2,3], and Tingmei Wang[1,2,3,*]

[1] Key Laboratory of Science and Technology on Wear and Protection of Materials, Lanzhou Institute of Chemical Physics, Chinese Academy of Sciences, Lanzhou 730000, China
[2] Center of Materials Science and Optoelectronics Engineering, University of Chinese Academy of Sciences, Beijing 100049, China
[3] State Key Laboratory of Solid Lubrication, Lanzhou Institute of Chemical Physics, Chinese Academy of Sciences, Lanzhou 730000, China

ABSTRACT

Designing high-performance microwave absorption materials become a prominent demand with the rapid development of information technology. In this work, needle-like morphology of aluminum nitride (AlN) decorated multi-walled carbon nanotubes (MWCNTs) as microwave absorbers has been successfully fabricated through a facile oil bath treatment. The MWCNTs/AlN composites exhibit outstanding microwave absorption performance with different content of MWCNTs, and the mass ratio of MWCNTs/AlN to paraffin is 2:3. The minimum reflection loss can reach to $-$ 47.34 dB at 9.12 GHz when the absorber thickness is 2.9 mm and the effective absorption bandwidth is 3.28 GHz with the composites containing 7 wt% MWCNTs. More importantly, the lowest density of MWCNTs/AlN composites can reach 0.316 ± 0.0294 g/cm^3, which is beneficial for practical applications. The significant improvement in microwave absorption properties of MWCNTs/AlN is major attributed to the enhancement of impedance matching, dielectric loss and multiple scattering by introducing different content of MWCNTs. This work might build an ideal to design novel lightweight, high-performance and broaden applications of microwave absorption materials, which can be widely used in practical fields under special conditions.

🖄 Springer

GRAPHICAL ABSTRACT
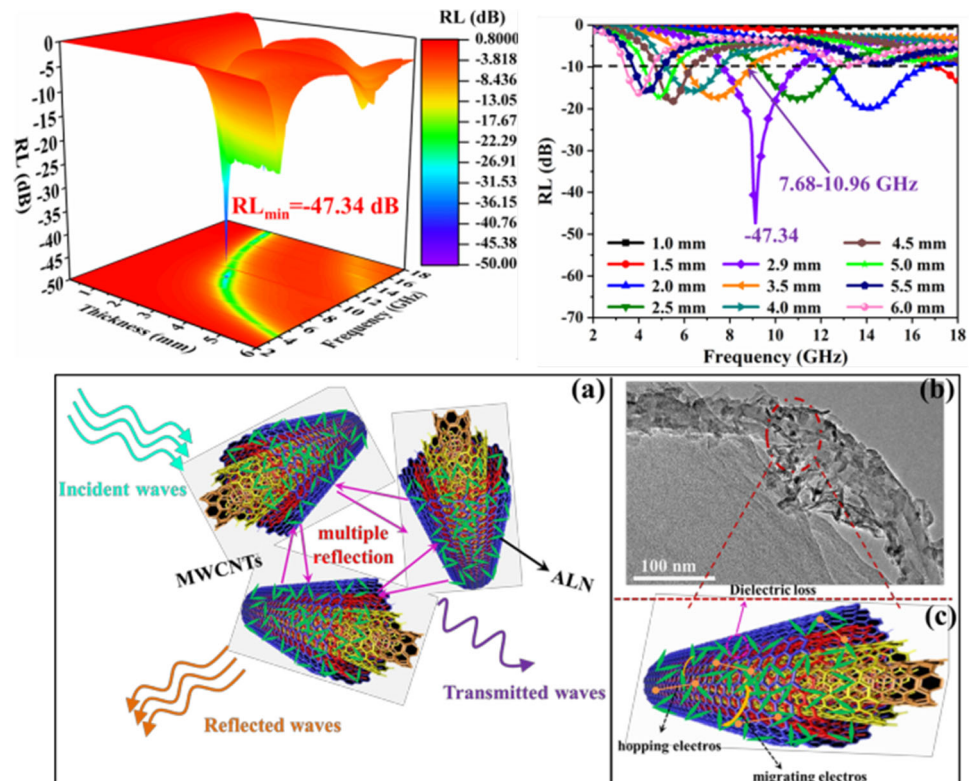
Introduction

Due to the development of anti-electronics devices, network technologies and small-scale communication equipment, much attention has been focused on microwave absorbing materials to solve the growing problems of electromagnetic interference and pollution, which could influence the property and widely applications of electronic equipment, even bring serious threats to information safety and the human health [1–4]. Although numerous remarkable accomplishments have been achieved by designing high-performance microwave absorbing materials, traditional microwave absorbing materials are still restricted in practical application due to their poor stability and high density. The ideal microwave absorbers require ultra-thin, lightweight, broad bandwidth and strong absorption [5–7].

Owing to excellent dielectric properties, carbon-based materials have attracted much attention in the last few years for the field of electromagnetic wave absorption application [8, 9]. Multi-walled carbon nanotubes (MWCNTs) as a typical one-dimensional carbon-based material, which possesses low density, high specific surface area and outstanding physical performance, have been widely studied as high-efficiency microwave absorbing material [10–12]. Nevertheless, the electromagnetic attenuation of MWCNTs caused by the single dielectric loss and the poor characteristic of synergistic effect requires improvement as microwave absorber [13–15].

In general, there are two criteria to evaluate a good microwave absorber: strong microwave absorption and broad bandwidth. Therefore, inducing magnetic nanoparticles onto or into the surface of MWCNTs is an effective approach to enhance the microwave absorption capacity of MWCNTs [16–21]. Li et al. [10]

fabricated the coated CNTs with optimized Fe_3O_4 nanocoating structure via solvothermal method and the RL_{min} reached -28.7 dB with the widest bandwidth of 8.3 GHz. Zhang et al. synthesized carbon-coated $RGO/CoFe_2O_4$ hollow particles-modified MWCNTs composites, and the corresponding RL bandwidth was 13.1 GHz with thickness from 1.2 to 4 mm [22]. Zhang et al. [23] fabricated a $CoFe_2O_4$/CNTs nanocomposite through solvothermal method. The results showed that RL of $CoFe_2O_4$/CNTs nanocomposites reached -15.7 dB with the bandwidth of 2.5 GHz when the solvothermal temperature increased to 260 °C. However, most of the reported materials show low resistance to severe conditions (high temperature, strong acid and alkali, high mechanical strength, etc.). Consequently, it is a promising and meaningful to design and fabricate novel microwave absorbing materials by choosing unconventional materials with excellent performance in other aspects.

Owing to low thermal expansion coefficient, high thermal conductivity and the strong resistance to molten metal erosion, aluminum nitride (AlN) as a good heat-resistant material has been attracted considerable interest in the fields of microelectronic and optoelectronic devices [24, 25]. Besides the thermal conductivity of MWCNTs and AlN as microwave absorber, the good dielectric property of AlN is rare reported [26]. Introducing AlN and the defects of MWCNTs are conducive to enhance dielectric, polarization and synergistic effect of MWCNTs/AlN composites, which might be beneficial to achieve the goal of ideal absorber design and be applied to more critical fields with relative restrict conditions.

In this work, we prepared MWCNTs/AlN composites with superior absorption performance by a one-step method. The results indicate that the RL_{min} value of MWCNTs/AlN composites reaches -47.34 dB at 9.12 GHz with a thickness of 2.9 mm and the effective absorption bandwidth is 3.28 GHz when the content of MWCNTs increases to 7 wt %. We proposed a possible microwave absorption mechanism for interfacial interaction and synergistic effect. This work may pave the way for designing novel absorbing materials with lightweight and high-performance.

Experimental section

Materials and reagents

All chemicals reagents in our experiment are analytical grade and used without further purification. DMF (N, N-Dimethylformamide) and absolute ethanol are provided from Li Anlong Pharmaceutical Chemical Reagent Co. Ltd (Tianjin, China). MWCNTs of 5–10 μm in length and 30–50 nm in diameter are purchased by Xianfeng nanomaterial science and technology Co. Ltd (Nanjing, China). AlN nanopowders with 5–10 nm in diameter and 80–120 nm in length are obtained from Chaowei nanotechnology Co. Ltd (Shanghai, China). In addition, absolute ethanol and deionized water were used to clean products.

Synthesis of MWCNTs/AlN composites

The fabrication of MWCNTs/AlN composites is illustrated in Fig. 1. The MWCNTs were treated by strong acid solution under stable ultrasonication to functionalize MWCNTs with –OH or -COOH. Afterward, the products were washed with deionized water till their pH value was close to 7, and then the functionalized MWCNTs were dried at 70 °C for 24 h. Next, different content of functionalized MWCNTs (20, 50, 70 and 100 mg) and AlN nanopowders (0.98, 0.95, 0.93 and 0.9 g) were dispersed into 300 mL dimethyl formamide (DMF) ultrasonication for 2 h. Thereafter, the dispersion was transferred to a flask with condenser and followed with stirring at 120 °C for 8 h. Finally, the precipitates were rinsed with deionized water and absolute ethanol many times and followed with drying in oven at 85 °C for 24 h, the MWCNTs/AlN composites were obtained.

Characterizations

X-ray diffractometer (X'Pert, NL) with Cu K α radiation ($\lambda = 1.541$ Å) was applied to analyze composition and phase structure of samples through X-ray diffraction (XRD) patterns. The morphology analyses were performed on transmission electron microscopy (TEM, TF20-FEI, USA) and scanning electron microscopy (SEM, JSM-5600LV, Japan). The chemical bonds of the samples were analyzed by Fourier transform infrared (FTIR) spectra within the range of
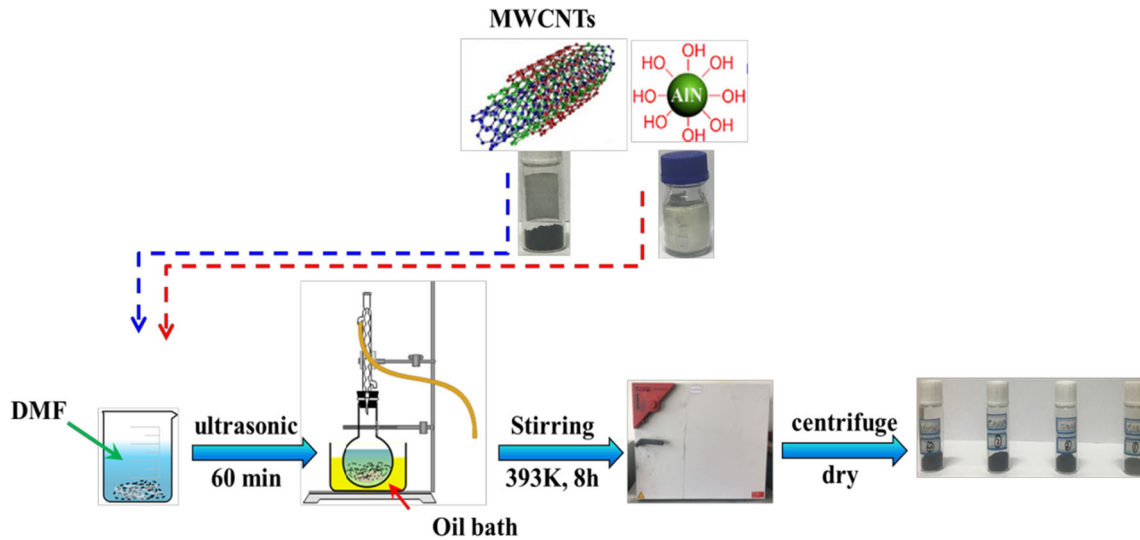
Figure 1 The synthesis schematic illustration for MWCNTs/AlN composites.

600–3600 cm^{-1}. The existing disordered and ordered crystal structures of carbon-based materials were tested by HR-800 Raman Spectrometer (HJY, FRA) equipped with a He–Ne Laser. The Brunauer–Emmet–Teller (BET) surface area was measured by N$_2$ adsorption–desorption isotherms.

Measurements of electromagnetic performance

The different contents of MWCNTs/AlN (0 {S-0}, 2 {S-2}, 5 {S-5}, 7{S-7} and 10 {S-10} wt%) were mixed through paraffin wax (2:3) and molded into cylindrical shape with outer and inner diameter of 7.00 mm and 3.04 mm. The relative permittivity $((\varepsilon_r = \varepsilon' - j\varepsilon''))$ and permeability $((\mu_r = \mu' - \mu''))$ as core index for electromagnetic parameters to estimate the absorption performance of composites. The complex permittivity (ε_r) and permeability (μ_r) of MWCNTs/AlN-paraffin samples were measured on a vector network analyzer (VNA, N5232B, Agilent) at room temperature with the transmission coaxial method in the range of 2–18 GHz.

Brief mechanism

A possible microwave absorption mechanism is depicted in Fig. 2. It is well known that a part of the incident electromagnetic waves cannot be absorbed on the surface of absorbing materials and other electromagnetic waves enter inside of materials

then occur multiple reflections and multiple scattering until are attenuated as possible and finally the surplus waves are transmitted. It is expected that the input impedance of materials can close to that of free space by design in order to improve the absorption efficiency of materials for electromagnetic wave energy [27]. The network structures of MWCNTs play a critical role in increasing transmission of electromagnetic waves due to the presence of effective permittivity. What's more, the "bridge-frame" connections between MWCNTs and AlN in the network structure might prolong the propagation paths for electromagnetic waves and improve the attenuate efficiency of the incident electromagnetic waves. The dielectric loss is normally considered composed of polarization loss and conductivity loss according to the Debye theory [28]. Herein, the interactions between MWCNTs and AlN interfaces lead to the appearance of the interfacial polarization and the surface functional groups could also induce the dipole polarization. In addition, MWCNTs/AlN composites can create conductive network environment for charges migrating and hopping.

Results and discussion

Figure 3 presents the XRD patterns of different content of MWCNTs/AlN samples. The diffraction peaks at $2\theta = 33.29°$, $36.15°$, $37.82°$, $49.89°$, $59.49°$, $66.04°$, $69.78°$, $71.51°$ and $72.68°$ of MWCNTs/AlN
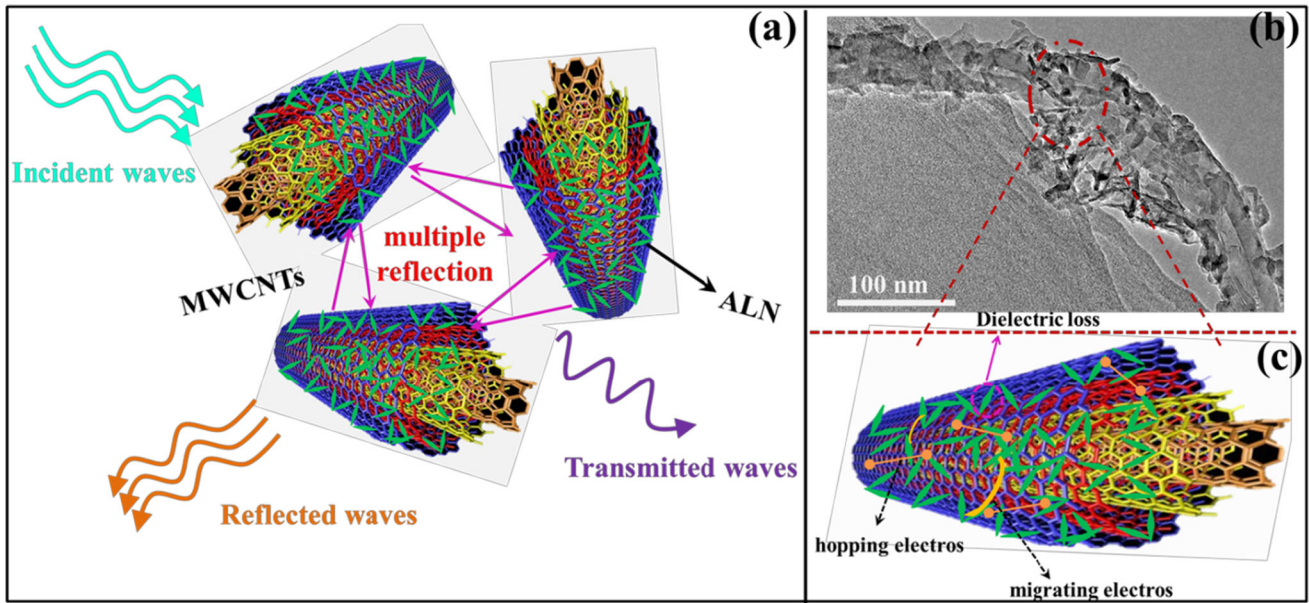
Figure 2 Schematic illustration of the possible electromagnetic wave absorption process in MWCNTs/AlN composite absorber **a** Multiple reflections and scatterings, **b** TEM image of MWCNTs/ AlN composite and **c** Interfacial polarization, dipole polarization and dielectric loss.
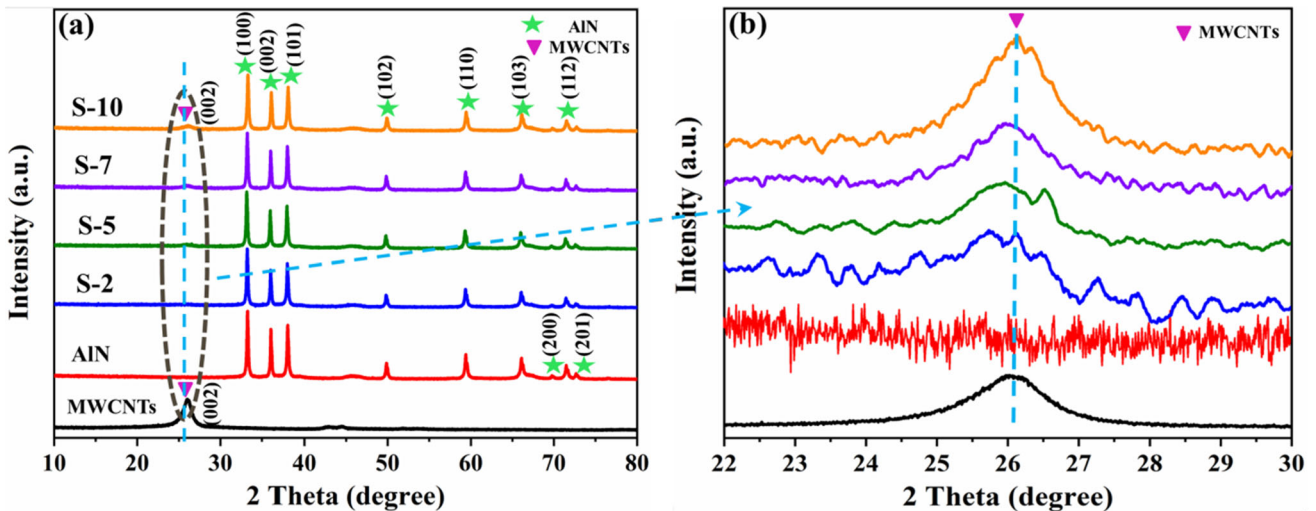

Figure 3 **a** XRD patterns and **b** the magnified peaks of different content of MWCNTs/AlN.

can be assigned to (100), (002), (101), (102), (110), (103), (200), (112) and (201) crystal planes of AlN (JCPDS No. 25–1133), respectively [29]. In addition, the characteristic diffraction peaks of MWCNTs at 26.17° which ascribe to (002) crystal planes (JCPDS No. 26–1076) are also observed in MWCNTs/AlN samples [30]. Figure 2b shows that the peak's intensity of MWCNTs/AlN increases with the increase in MWCNTs content. Besides MWCNTs and AlN patterns, no other diffraction peaks are found, it

demonstrates the obtained composites maintained the individual phase as prepared [31].

Figure 4 displays the microscopic morphology of different content of MWCNTs/AlN samples. As shown in Fig. 4a, SEM images of pure MWCNTs exhibit the typical tube structure with diameter of 30–50 nm. Figure 4b demonstrates the nano-scale AlN are densely stacked with irregular distribution. Figure 4c–d shows the morphology of sample of S-7. The AlN nanoparticles are decorated on the
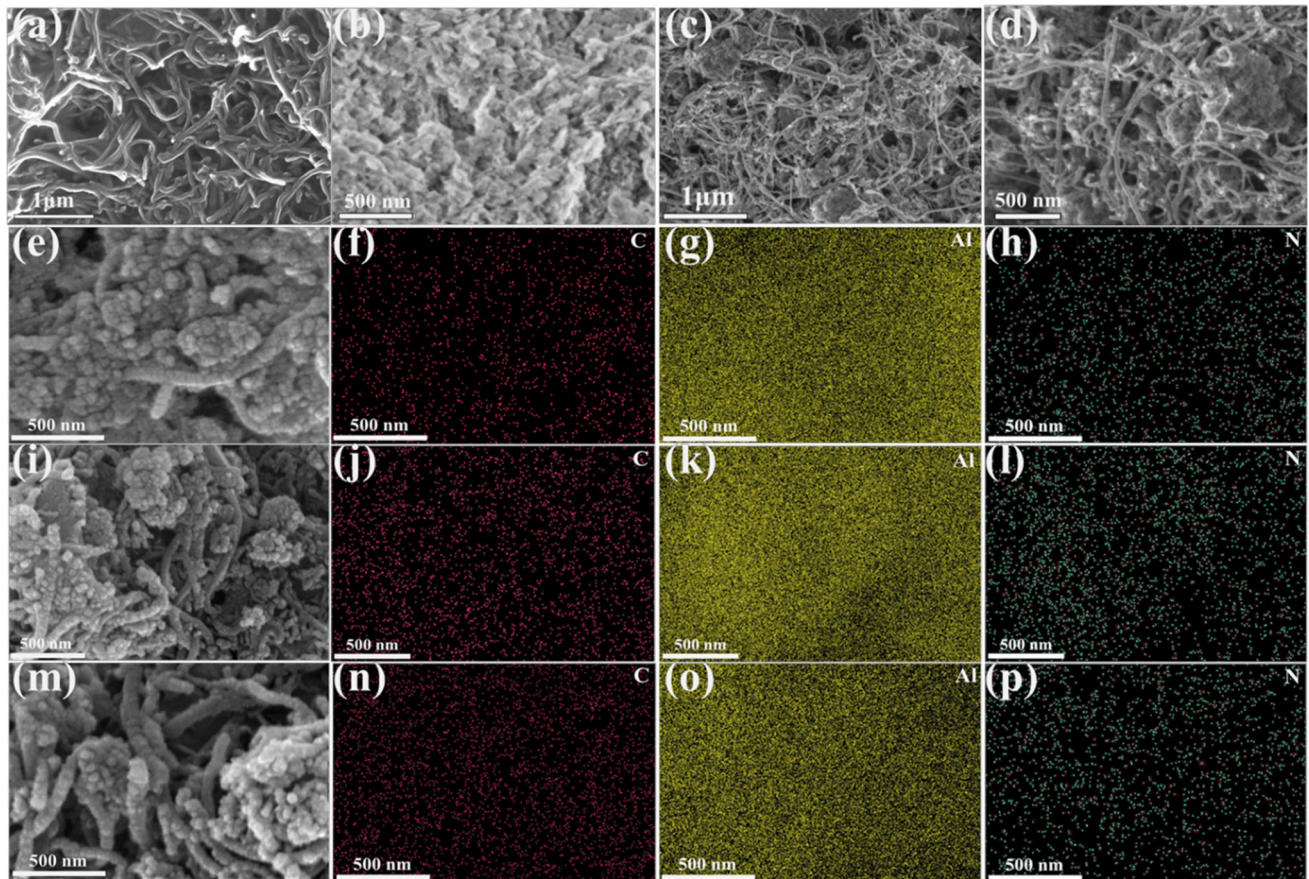
Figure 4 SEM images of **a** MWCNTs, **b** AlN, **c**, **d** S-7, **e** S-2, **i** S-5, **m** S-10 and the corresponding EDS images of S-2 (**f**–**h**), S-5 (**j**–**l**) and S-10 (**n**–**p**).

surface of MWCNTs, part of the AlN plays a role of junctions to connect the neighboring MWCNTs and yield the network. Besides, the morphologies of S-2, S-5 and S-10 are also presented in Fig. 4e, i, m for comparison. It can be clearly observed that the presence of MWCNTs is increasing and the increase in the twining degree may change the path of charges propagation in the composites. Energy-dispersive X-ray spectroscopy (EDS) is performed to identify the element distribution and chemical compositions of the samples. Figure 4(f–h), (j–l) and (n–p) shows the distribution of C, Al and N elements in S-2, S-5 and S-10, respectively, it demonstrates successful synthesis of MWCNTs/AlN, which is consistent with the XRD data. The formed MWCNTs network structures through AlN might enhance the electrical conductivity due to the formed conductive paths and it could potentially improve the permittivity and allow MWCNTs/AlN composites to perform an excellent property of microwave absorption.

The microscopical and morphology of MWCNTs, AlN and MWCNTs/AlN (S-2, S-5, S-7 and S-10) composites are studied by TEM. Figure 5a–b clearly shows typical tube structure of the MWCNTs with the outer and inner cavities diameter of 40–45 and 8–16 nm, respectively. Figure 5c shows the needle-like morphology of AlN nanoparticles with the length of about 100 nm and a diameter ranging from 5 to 10 nm. For S-5 (Fig. 5d-f), it shows that the surface of MWCNTs is attached with slightly agglomerated AlN, it is attributed to chemical bonds between MWCNTs and AlN. For comparison, Fig. 5 g–i presents the morphology of S-2, S-5 and S-10, respectively. It reconfirms that the gradually increased content of MWCNTs results in the serious twining and stacking. Meanwhile, AlN with different degree of agglomerate is not uniformly decorated on the surface of MWCNTs. These modifications are harmful to the free-transfer of electrons and decrease the dielectric loss properties of composites. The results indicate that the conductive matrix of
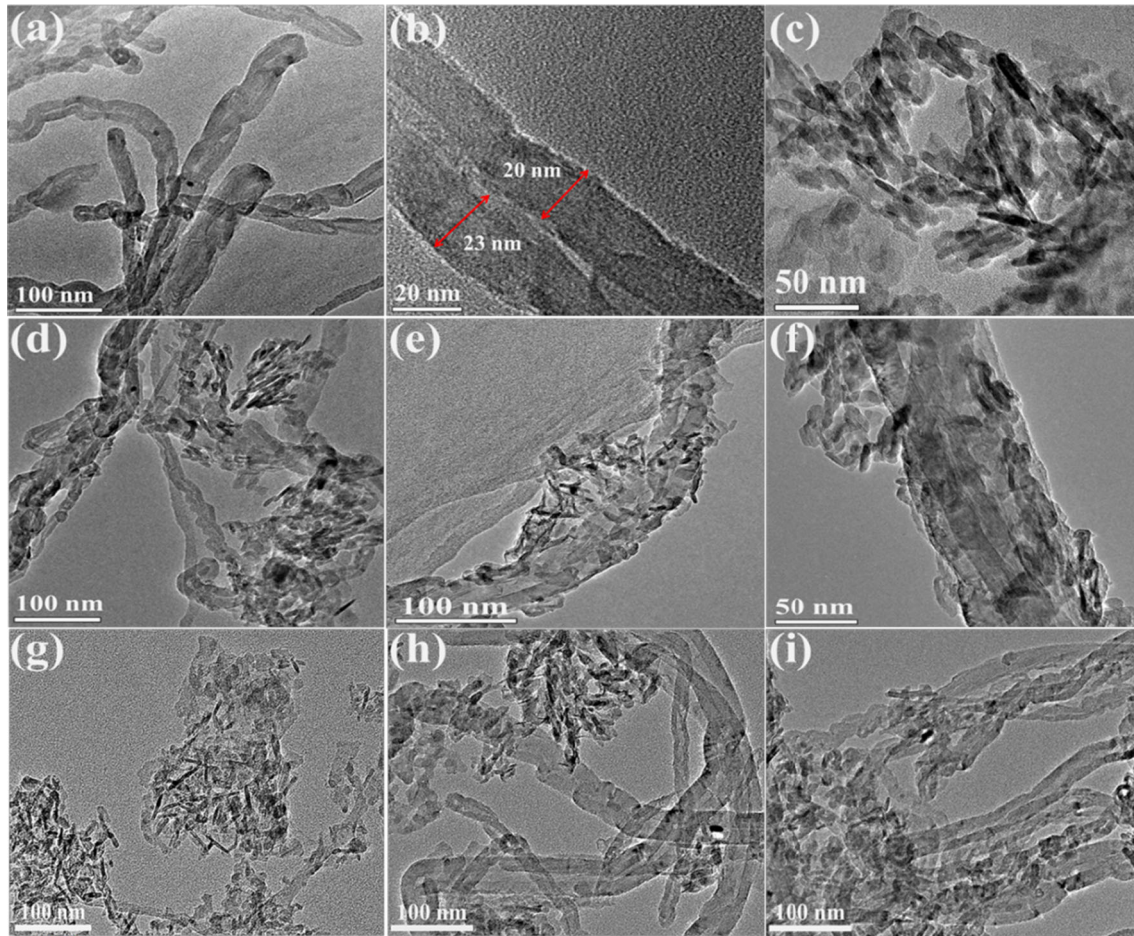
Figure 5 TEM images of **a**, **b** MWCNTs, **c** AlN, **d**–**f** S-7, **g** S-2, **h** S-5 and **i** S-10.

MWCNTs could tune the dielectric loss performance and determine the final absorption property of MWCNTs/AlN composites with the proper content of MWCNTs.

The densities ρ of the as-prepared samples can be calculated by the formula: $\rho = m_1/v$, $v = (m_1-m_2)/\rho_{water}$ and the density of deionized water used is defaulted to 1 g/cm^3 in this density measurement where m_1 and m_2 are regarded as the weights of equivalent products in air and in deionized water. Figure 6a shows the densities of MWCNTs, AlN, S-2, S-5, S-7 and S-10. Obviously, AlN has the lowest density, which is 0.850 ± 0.0154 g/cm^3, and the densities of MWCNTs/AlN samples gradually increase as the content of MWCNTs increases in the final composites. The density of S-2 is 0.683 ± 0.0184 g/cm^3, which the density of S-10 is 0.316 ± 0.0294 g/cm^3. These results indicate that the densities of the as-obtained samples can be easily adjusted through changing the content of MWCNTs

in the MWCNTs/AlN composites. The specific surface areas of S-2, S-5, S-7 and S-10 are measured by the N$_2$ adsorption–desorption isotherms. As presented in Fig. 6b, the specific surface area of S-2, S-5, S-7 and S-10 is 45.66, 57.31, 59.32 and 61.72 m^2/g, respectively. This tendency is major attributed to the increased content of MWCNTs and their high specific surface area. The result indicates that the good stability of MWCNTs/AlN morphology with the different content of MWCNTs is beneficial for the enhancement of microwave absorption performance of MWCNTs/AlN composites.

Figure 7a shows the Raman spectra of MWCNTs, AlN and MWCNTs/AlN (S-2, S-5, S-7 and S-10) composites in the range of 500–3500 cm^{-1}. For MWCNTs, there are three dominant Raman peaks at 1332, 1579 and 2651 cm^{-1}, which are corresponding to the first-order vibration of sp^3 (D band), the second-order vibration of sp^3 (G band) and the in-plane vibration of sp^2 bond (2D band), respectively [16].

(a)

(b)
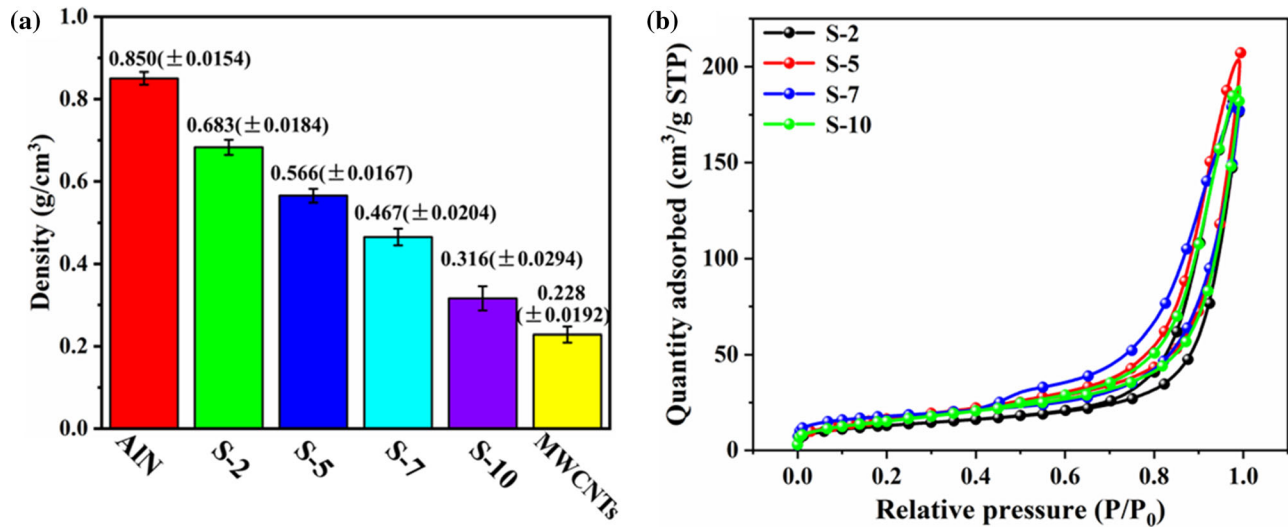
Figure 6 **a** Densities of MWCNTs, AlN, S-2, S-5, S-7 and S-10; **b** N_2 adsorption–desorption isotherm of S-2, S-5, S-7 and S-10.

The values of I_D/I_G for S-2, S-5, S-7 and S-10 are 0.77, 0.79, 0.81 and 0.82, respectively, which are stronger than that of MWCNTs (I_D/I_G = 0.69). The increase in I_D/I_G values indicates the reducing of average size sp^3 and the enlarging of defects and disorder degree of MWCNTs/AlN composites with the increase in MWCNTs content, which are beneficial to the enhancement of conductivity properties [11]. Besides, three Raman peaks are observed at 613, 652 and 689 cm^{-1}, which correspond to the A_1(TO), E_2(high) and E_1(TO) modes of AlN [32]. Significantly, the Raman peaks (D, G and 2Ds) of the MWCNTs/AlN composites compared with MWCNTs and AlN slightly right shift, which indicates charges redistribution on some interfaces. This is attributing to the needle-like AlN attached onto the surface of MWCNTs [12].

FTIR is an influential technique to explain the changes in chemical structures. Figure 7b–c displays the FTIR spectra of MWCNTs, AlN and MWCNTs/AlN (S-2, S-5, S-7 and S-10) composites within 3600–600 cm^{-1}. The asymmetric strong and broad band between 3000 and 3595 cm^{-1} belongs the stretching vibration of O–H band from carboxylic groups and adsorbed water molecules on the surface of MWCNTs. The functionalized MWCNTs present characteristic graphite structure peak at 1630 cm^{-1} [33]. Besides, a peak at 1072 cm^{-1} can be ascribed to the stretching of carbonyl groups (C=O). The pristine AlN exhibits two strong characteristic peaks at around 710 and 3456 cm^{-1}, which belongs to the

vibration of AlN band and the stretching vibration of hydroxyl group (–OH), respectively. In addition, a weaker peak at about 1641 cm^{-1} belongs to in-plane deformation of –N–H–, which suggests a high reactivity and affinity to water of AlN [29, 34]. For MWCNTs/AlN (S-2, S-5, S-7 and S-10) composites, the presence of peaks includes all the characteristic peaks both MWCNTs and AlN and the corresponding intensity of peaks become much strong with the increase in MWCNTs content. Moreover, two peaks at around 2917 and 2856 cm^{-1} correspond to asymmetric and symmetric stretching vibrations of υ_{as}(-CH_2) and υ_s(CH_2) of MWCNTs [35]. These characteristic peaks prove that AlN has been grafted on the surface of MWCNTs, which may play a critical role in absorption performance of the products.

The microwave absorption performance of materials is normal estimated by the relative complex permeability ($\mu_r = \mu' - \mu''$) and permittivity ($\varepsilon_r = \varepsilon' - j\varepsilon''$). The real $\varepsilon'$and imaginary ε''parts of MWCNTs, AlN and MWCNTs/AlN composites with the different content of MWCNTs are displayed in Fig. 8. From Fig. 8a, b, the relative permittivity values of MWCNTs, AlN and MWCNTs/AlN composites keep a decreasing tendency with the increase in frequency in the range of 2–18 GHz. Furthermore, the complex permittivity values of MWCNTs/AlN composites are less than that of pure MWCNTs, indicating the introduction of AlN can reduce the ε_r values. Besides, the ε' values of S-7 decline from 13.7 to 10.2 within the range of 2–8.5 GHz and then the
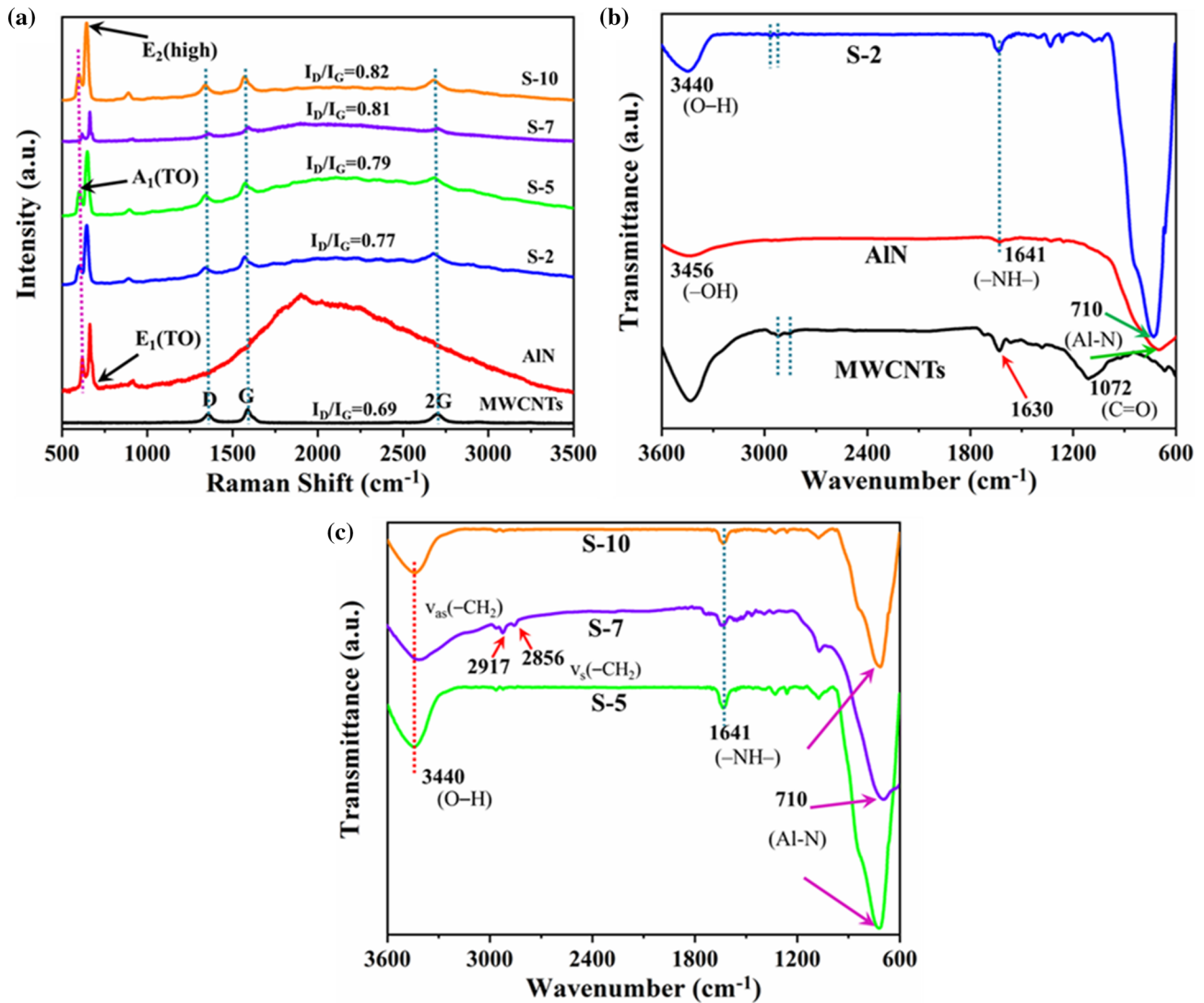
Figure 7 **a** Raman and **b**, **c** FTIR spectra of MWCNTs, AlN and MWCNTs/AlN (S-2, S-5, S-7 and S-10) composites.

value of ε' gradually increases till 10.4 GHz to achieve the maximum of 10.8. Later on, ε' decreases over the range from 10.4–14.8 GHz and remains till 18 GHz. For S-2, S-5 and S-10, ε' decreases from 5.8 to 5.2, 12.3 to 5.6 and 17.5 to 9.1, respectively, over the whole frequency range. Figure 8b presents the ε'' values of S-7 declines from 6.2 to 3.3 with fluctuations at some frequencies and similar trends are also observed in S-5 and S-10, while S-2 almost keeps a constant approximate 0.4 in the range of 2–18 GHz. We all know that the dielectric loss is an important factor to estimate the microwave absorption performance of materials. The dielectric loss tangents $\tan \delta_\varepsilon = \varepsilon_r''/\varepsilon_r'$ are presented in Fig. 8c. The dielectric loss of MWCNTs/AlN composites gradually increases with the change of AlN content, indicating that

the dielectric loss is improved due to the introduction of proper content of AlN. The results suggest that AlN-modified MWCNTs play a critical role in the conductive behavior, proper content of MWCNTs is the major effect on the response performance of the electrical component to determine the absorption properties of composites within the measured frequency. In addition, the real permeability (μ') is regarded as 1, while the imaginary permeability μ'' is close to 0 due to no magnetic materials are additive in the composites and it also implies that the magnetic loss is negligible toward the incident electromagnetic wave.

Debye dipole relaxation based on the calculated results of the permittivity responses is used to determine the contribution to the loss behavior of
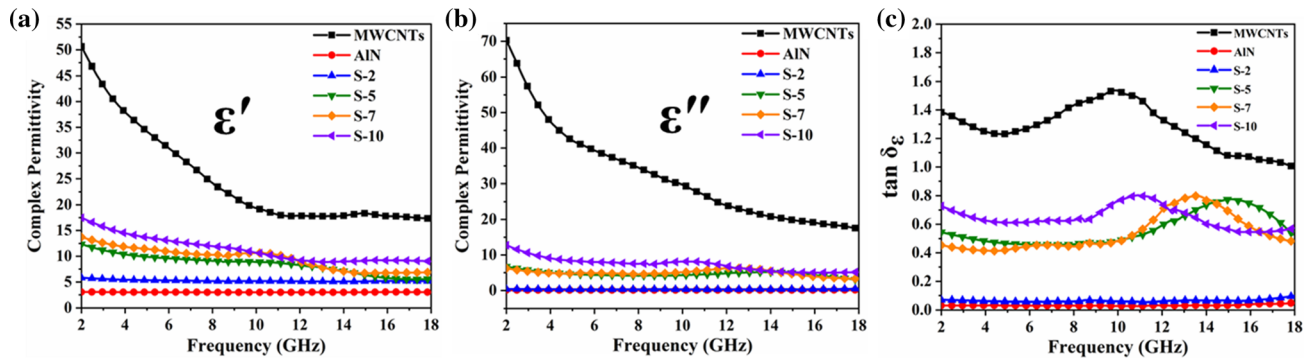
Figure 8 Frequency dependence of **a** real, **b** imaginary parts of relative complex permittivity and **c** dielectric loss of MWCNTs, AlN, S-2, S-5, S-7 and S-10.

dielectric component in the microwave absorber. Debye dipolar relaxation is often considered as the mainly exist in dielectric interaction and estimated by Cole–Cole semicircles, as shown in the following equations [15, 36]:

$$\varepsilon_r = \varepsilon_\infty + \frac{\varepsilon_s - \varepsilon_\infty}{1 + j2\pi f\tau} = \varepsilon' - j\varepsilon'' \tag{1}$$

Here, in ε_S, ε_∞ τ and f refer to the static permittivity, relative dielectric permittivity at high-frequency limit, polarization relaxation time and frequency, respectively. Meanwhile, ε' and ε'' can be specifically expressed as the following equations:

$$\varepsilon' = \varepsilon_\infty + \frac{\varepsilon_s - \varepsilon_\infty}{1 + (2\pi f)^2\tau^2} \tag{2}$$

$$\varepsilon'' = \frac{2\pi f\tau(\varepsilon_s - \varepsilon_\infty)}{1 + (2\pi f)^2\tau^2} \tag{3}$$

By further simplifying, the relationship between ε' and ε'' can be depicted as following:

$$\left(\varepsilon' - \frac{\varepsilon_s + \varepsilon_\infty}{2}\right)^2 + (\varepsilon'')^2 = \left(\frac{\varepsilon_s - \varepsilon_\infty}{2}\right)^2 \tag{4}$$

The plots of ε'' vs. ε' reveal the obvious change in loss permittivity and confirm Debye relaxation as a major reason for dielectric effect, as presented in Fig. 9a–f. For the Cole–Cole plots of MWCNTs and AlN, it can be obviously seen that the existence of one semicircle at most due to conduction loss plays major role in dielectric loss. Besides, the distorted semicircles suggest that other effects including conductive loss, interfacial polarization and oxygen defects may also contribute to the microwave absorption property [37]. With the increase in the electromagnetic field, the semicircle radius of the second stage is reduced due to the damage of the lattice. The defect of

MWCNTs/AlN composites increases with the increase in content of MWCNTs to 7%, and the dielectric relaxation process becomes less obvious, which caused by the hysteresis of the induced charge. Based on Debye theory, ε'' includes conduction and the relaxation loss [38]. Cao et al. reported the electron-hopping model, the electrons can migrate or jump to the reduce graphene oxide (RGO) sheets or MWCNTs through the defects or interfaces between RGO sheets or MWCNTs when microwaves penetrate into the hybrid nanocomposites [39]. It is certain that the occurred Debye relaxation could affect the dielectric relaxations through the interactions between MWCNTs and AlN [27, 40, 41]. The results confirm that the various RL values of samples with different content of MWCNTs are determined by Debye relaxation effects.

Normally, the electromagnetic absorption properties of absorbers are depicted by the reflection loss (RL) values. RL is calculated according to following equations [40, 41]:

$$RL(dB) = 20\log\left|\frac{Z_{in} - Z_0}{Z_{in} + Z_0}\right| \tag{5}$$

$$Z_{in} = Z_0\sqrt{\frac{\mu_r}{\varepsilon_r}}\tanh\left[j\left(\frac{2\pi fd}{c}\right)\sqrt{\mu_r\varepsilon_r}\right] \tag{6}$$

According to Eq. (6), if Z_{in} is closer to Z_0, the better impedance matching could be obtained and it could improve the microwave absorption properties of MWCNTs/AlN composites as absorbers. Herein, Z_{in} is the input impedance of absorber, Z_0 is the impedance of free space, f is frequency, d is thickness of the samples, c is the velocity of electromagnetic wave in free space. In order to further study the relationship between RL values and the impedance of the
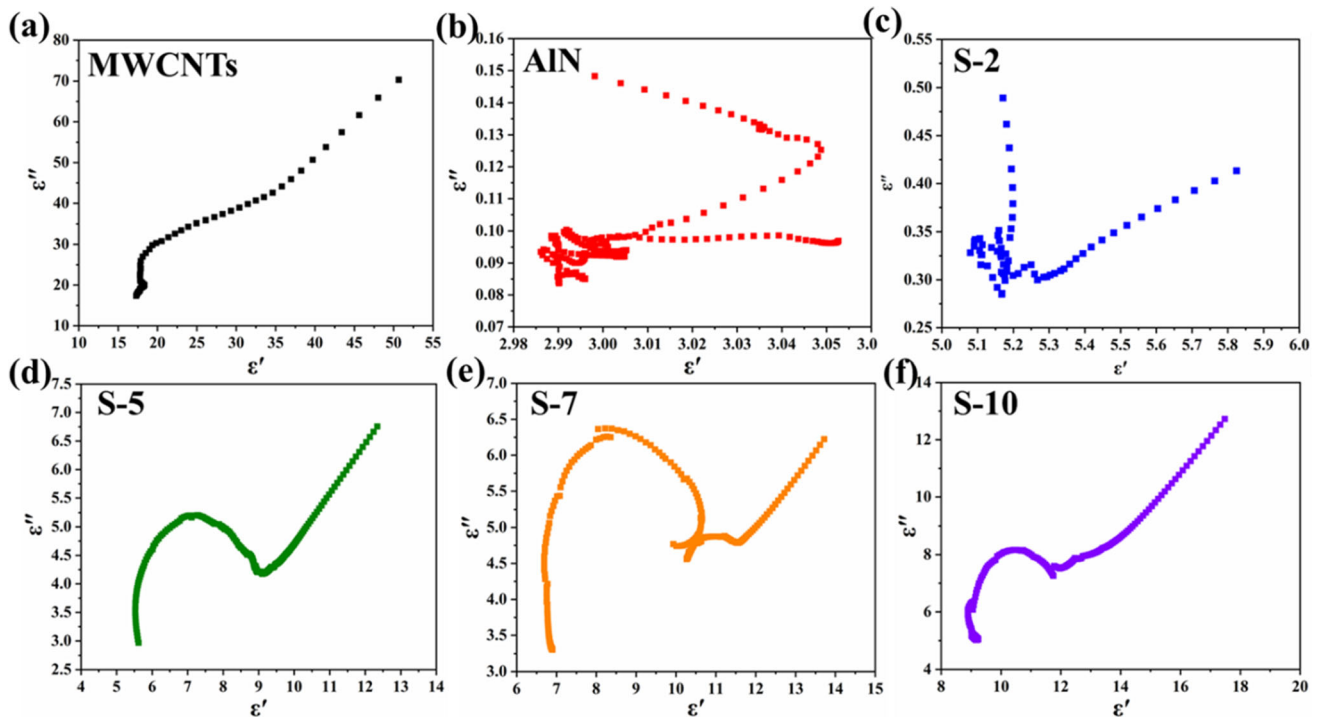
Figure 9 a–d Cole–Cole semicircles (ε'' vs. ε'): **a** MWCNTs, **b** AlN, **c** S-2, **d** S-5, **e** S-7 and **f** S-10.

samples, Fig. 10 displays the relationship between Z_{in} and Z_0 of AlN-, MWCNTs-, S-2-, S-5-, S-7- and S-10-based absorbers with different thicknesses. The brown horizontal line in Fig. 10 indicates that value of Z_{in}/Z_0 is 1 and if the distance among the as-prepared samples is closer to the brown line, the corresponding impedance matching is a better one. As shown in Fig. 10a, b, both the Z values of AlN and pure CNTs are all far from 1 and the highest Z_{in}/Z_0 value is about 10.8 and 0.43, respectively, proving that the impedance matching performance of AlN and MWCNTs is the weakest. From Fig. 10c, the Z_{in}/Z_0 values of S-2 are far from 1 and the highest Z_{in}/Z_0 value is 3.7, proving that the impedance matching property of S-2 is the poorest. With the increase in AlN content, the Z_{in}/Z_0 values of S-5 (Fig. 10d) can be significantly improved. The best Z_{in}/Z_0 value is the closest to 1 at around 7 GHz at 3.5 mm. As shown in Fig. 10e, the Z_{in}/Z_0 values of almost all thicknesses of S-7 are very close to 1 and the best Z_{in}/Z_0 value is closest to 1 at frequency around 8 GHz at a thickness of 3.0 mm and it can be assumed that the best RL should appearance at this situation around. As can be seen from Fig. 10f, the Z_{in}/Z_0 values of S-10 are far from 1 except the relative better Z_{in}/Z_0 value is 1.2 at around 15 GHz at 1.5 mm, and the impedance matching values get worse with the further increase in AlN content. Therefore, the impedance matching

values of samples can be obviously improved with proper AlN content and they play an important role in improving the properties of microwave absorption in MWCNTs/AlN composites as absorbers.

Figure 11 displays the electromagnetic absorption properties of AlN, MWCNTs, S-2, S-5, S-7 and S-10 at thicknesses of 1.0–6.0 mm. As shown in Fig. 11a, b, c and d, the RL_{min} values of AlN and MWCNTs are less than -3 and -8 dB with all thicknesses, respectively, which confirm poor microwave absorption performance of AlN and pure MWCNTs. Figure 11e–f displays the RL values of S-2 versus frequency, which are tunable through changing thickness of the samples. The value of RL_{min} reaches to -21.65 dB at 17.12 GHz with a thickness of 5.9 mm. Result indicates that certain amount of AlN can significantly improve the absorption properties of MWCNTs, which attributes to the dielectric property of AlN. Figure 9g–h shows the RL_{min} of S-5 reaches -41.37 dB at 7.44 GHz with a thickness of 3.4 mm. Figure 9i–j presents the optimal RL_{min} value of S-7 is -47.34 dB at 9.12 GHz with a thickness of 2.9 mm and the effective absorption bandwidth is 3.28 GHz (7.68–10.96 GHz). Moreover, the whole frequency range (3.5–18 GHz) can be covered with corresponding effective absorption bandwidth through choosing proper thickness of the sample. However, barely absorption performance is obtained from the
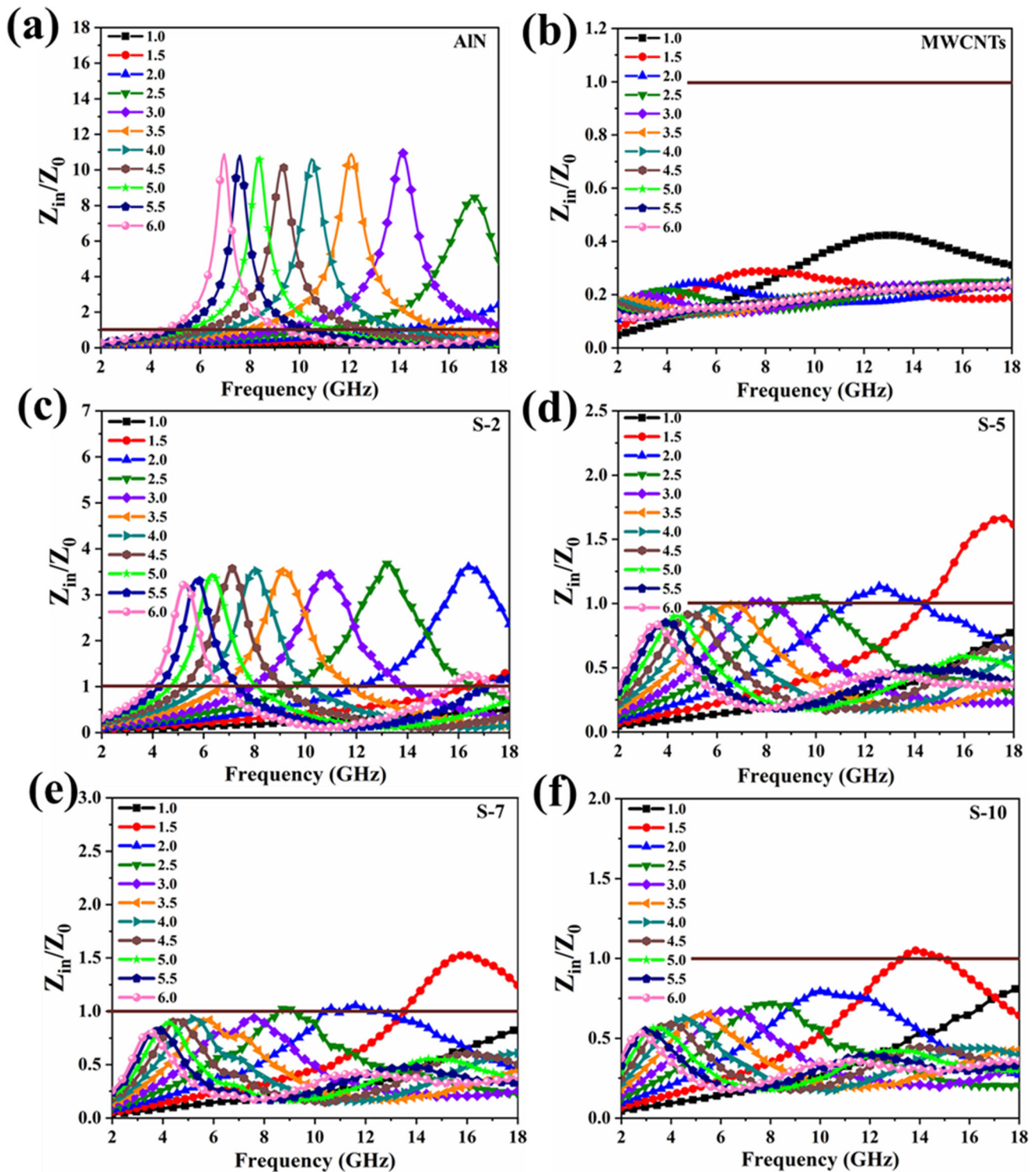
Figure 10 The relationship between Z_{in} and Z_0 of **a** AlN-, **b** MWCNTs-, **c** S-2-, **d** S-5-, **e** S-7- and **f** S-10-based absorbers with different thicknesses.

sample with a thickness of 1.0 mm. This kind of composite demonstrates that microwave absorption properties are different with thicknesses of absorbers.

As can be seen from Fig. 9k–l, S-10 value of RL_{min} is − 27.58 dB at 14.72 GHz with a thickness of only 1.6 mm, which indicates the microwave absorption

Figure 11 Microwave absorption properties of the as-prepared samples based absorbers: **a**, **b** AlN, **c**, **d** MWCNTs, **e**, **f** S-2, **g**, **h** S-5, **i**, **j** S-7 and **k**, **l** S-10.
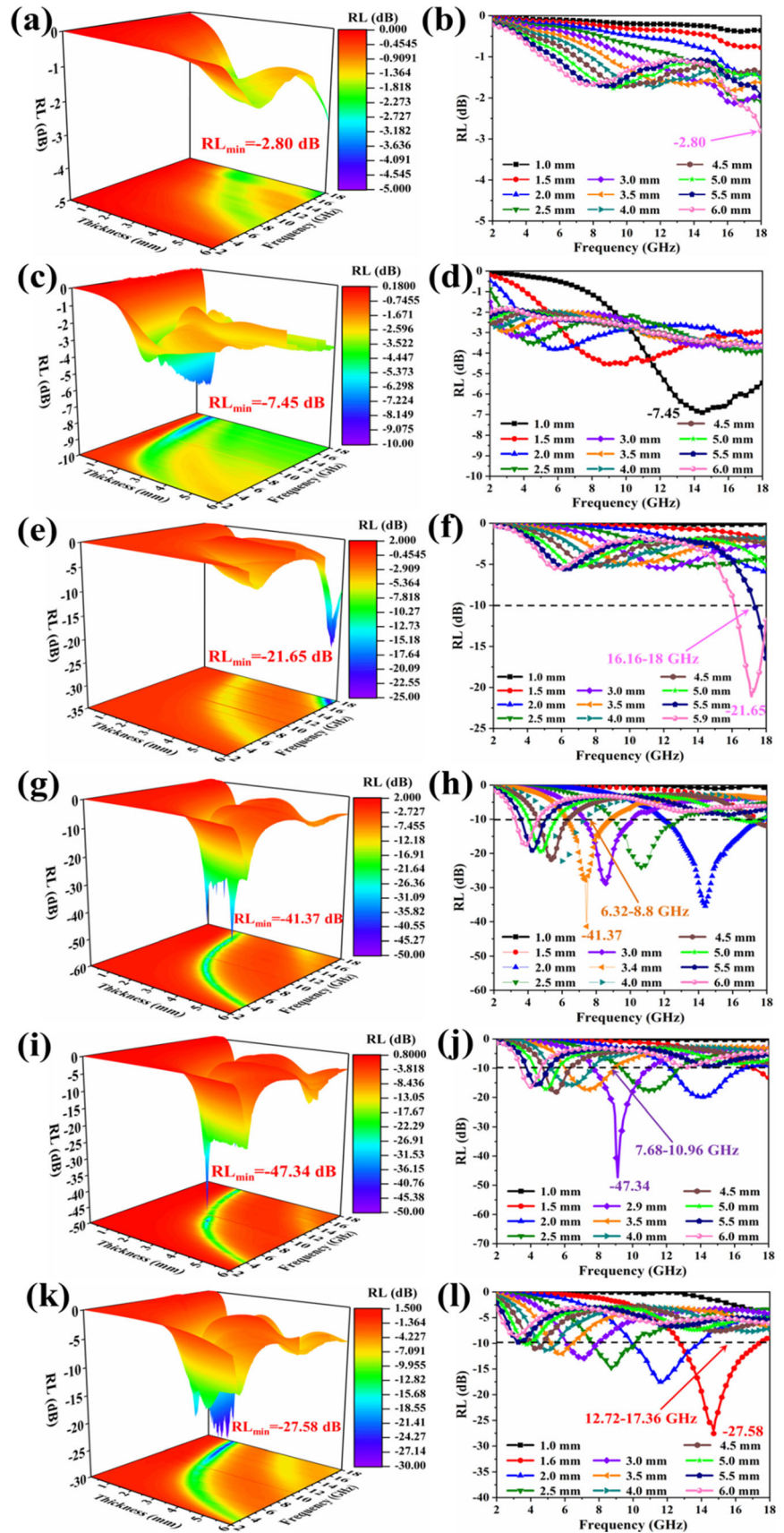
property of S-10 is weaker than that of the sample of S-5 and S-7. The results clarify that both the needle-like AlN and proper content of MWCNTs

Table 1 The microwave absorption results of AlN, MWCNTs, S-2, S-5, S-7 and S-10

Samples	RL_{min} (dB)	Thickness (mm)	Bandwidth (GHz)
AlN	− 2.80	6.0	0
MWCNTs	− 7.45	1.0	0
S-2	− 21.65	5.9	1.84
S-5	− 41.37	3.4	2.48
S-7	− 47.34	2.9	3.28
S-10	− 27.58	1.6	4.64

significantly affect the electromagnetic wave absorption property of MWCNTs/AlN composites. What's more, the electromagnetic wave absorption ability of the products reduces when the content of MWCNTs exceeding to 7%. The reason may be attributed to the weakening of the binding force between MWCNTs and AlN. With further increase in AlN agglomeration onto the surface of MWCNTs, the modified network structure of MWCNTs/AlN composites is hard to form due to the increase in the intertwining and deformation between MWCNTs and all of the results is consistent with the impedance matching changes of the as-obtained samples. Besides, all the microwave absorption properties of the samples including RL_{min},
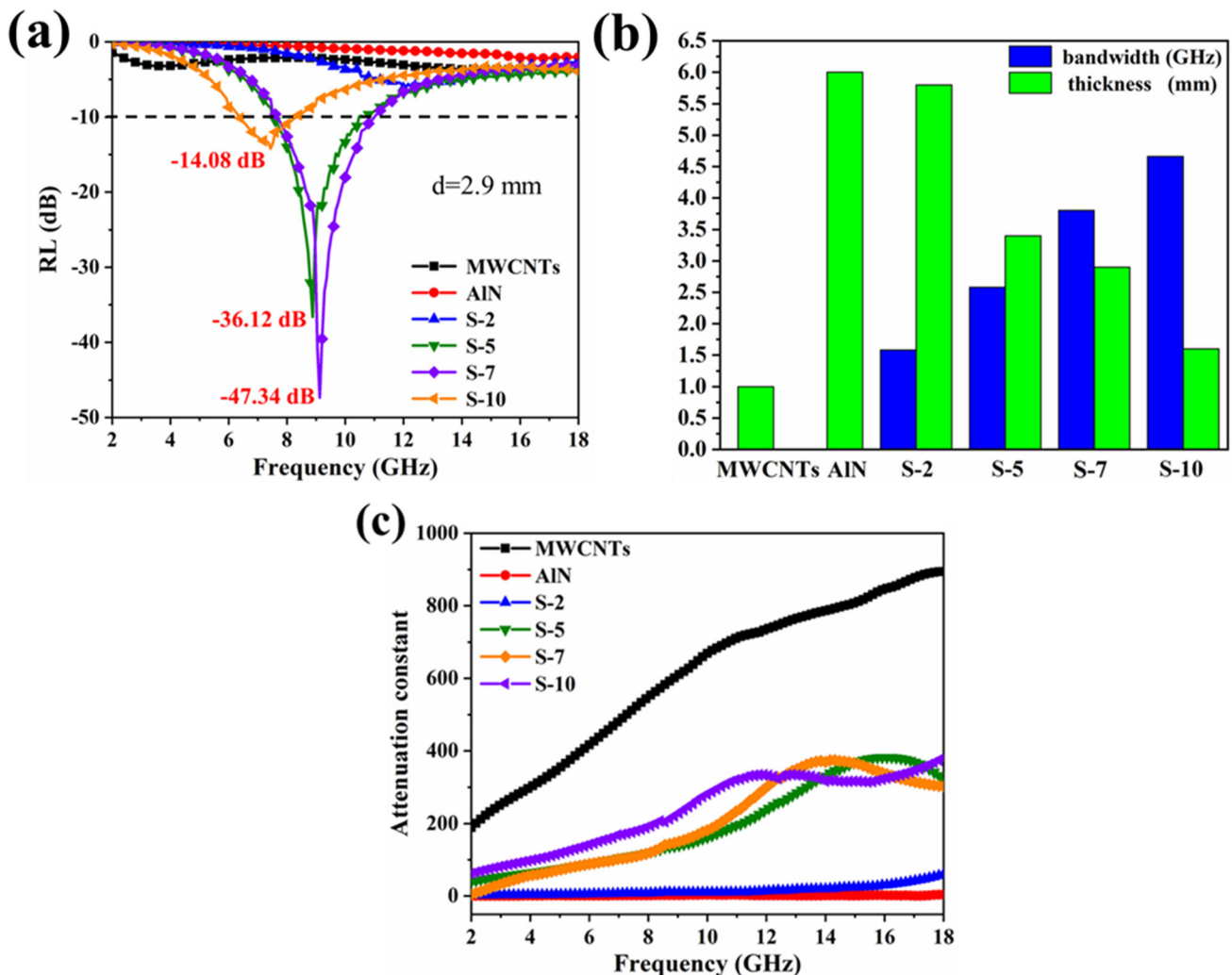
Figure 12 a Frequency dependence of reflection loss of MWCNTs, AlN, S-2, S-5 and S-7 and S-10 samples with a thickness of 2.9 mm, **b** effective bandwidths and thicknesses corresponding to the best RL values of the as-obtained samples and **c** the corresponding attenuation constants.

thickness and the effective bandwidth are summarized in Table 1.

To compare the electromagnetic wave absorption property of MWCNTs, AlN, S-2, S-5, S-7 and S-10, the related RL with a thickness of 2.9 mm is chosen and the results are shown in Fig. 12a. The RL_{min} values of S-5, S-7 and S-10 with the thickness of 2.9 mm are -36.12, -47.34 and -14.08 dB, respectively. On contrary, MWCNTs, AlN and S-2 show little RL values, and the results show that it is meaningful to prepare MWCNTs/AlN composites with different MWCNTs contents to further study the microwave absorption properties of samples. Figure 12b presents effective bandwidths and thicknesses corresponding to the best RL values of the as-obtained samples. Normally, the strong microwave attenuation capacity is also determined by microwave absorbers. According to the transmission line theory, the microwave attenuation abilities of materials can be required by the attenuation constant (α), which are calculated as the followed equation [42, 43]:

$$\alpha = \frac{\sqrt{2}\pi f}{c}$$
$$\times \sqrt{(\mu''\varepsilon'' - \mu'\varepsilon') + \sqrt{(\mu''\varepsilon'' - \mu'\varepsilon')^2 + (\varepsilon'\mu'' + \varepsilon''\mu')^2}}$$

$$(7)$$

The relationship between attenuation constant α and frequency of MWCNTs, AlN, S-2, S-5, S-7 and S-10 is illustrated in Fig. 12c. Obviously, the MWCNTs have the largest α values. However, the corresponding impedance matching is very poor in 2–18 GHz and thus the microwave absorption performance of MWCNTs is significantly weak. Besides, the α values of S-7 are higher than those of AlN, S-2, S-5 and S-10 within the range of 2–18 GHz, indicating that S-7 possesses the best microwave absorption owing to moderate impedance matching and strong attenuation loss, which is consistent with the results of RL.

Conclusion

In this work, MWCNTs/AlN network structured composites have been successfully synthesized by a facile method. The results show that different content of MWCNTs and needle-like AlN can significantly affect the microwave absorption property. S-7 exhibits the optimum RL_{min} value, it can reach to

-47.34 dB at 9.12 GHz with a thickness of 2.9 mm and the effective absorption bandwidth of 3.28 GHz. The outstanding microwave absorption property is ascribed to the modified network structure, the content of MWCNTs and synergistic effect between MWCNTs and AlN. It is expected that carbon-based/AlN composites might be powerful absorbing materials with ultra-thin thickness, wide bandwidth and high-efficient performance and widely used in practical fields.

Compliance with ethical standards

Conflict of interest   The authors declare no conflict of interest.

References

[1] Zhu W, Wang L, Zhao R, Ren J, Lu G, Wang Y (2011) Electromagnetic and microwave-absorbing properties of magnetic nickel ferrite nanocrystals. Nanoscale 3(7):2862–2864

[2] Wang Y, Chen D, Yin X, Xu P, Wu F, He M (2015) Hybrid of MoS_2 and reduced graphene oxide: a lightweight and broadband electromagnetic wave absorber. ACS Appl Mater Interfaces 7(47):26226–26234

[3] Liu J, Cao M, Luo Q, Shi H, Wang W, Yuan J (2016) Electromagnetic property and tunable microwave absorption of 3D nets from nickel chains at elevated temperature. ACS Appl Mater Interfaces 8(34):22615–22622

[4] Xi J, Zhou E, Liu Y, Gao W, Ying J, Chen Z, Gao C (2017) Wood-based straightway channel structure for high performance microwave absorption. Carbon 124:492–498

[5] Zhang Y, Huang Y, Zhang T, Chang H, Xiao P, Chen H, Huang Z, Chen Y (2015) Broadband and tunable high-performance microwave absorption of an ultralight and highly compressible graphene foam. Adv Mater 27(12):2049–2053

[6] He J, Wang X, Zhang Y, Cao M (2016) Small magnetic nanoparticles decorating reduced graphene oxides to tune the electromagnetic attenuation capacity. J Mater Chem C 4(29):7130–7140

[7] Liu P, Ng V, Yao Z, Zhou J, Lei Y, Yang Z, Lv H, Kong L (2017) Facile synthesis and hierarchical assembly of flower-like NiO structures with enhanced dielectric and microwave absorption properties. ACS Appl Mater Interfaces 9(19):16404–16416

[8] Sun Y, Xu J, Qiao W, Xu X, Zhang W, Zhang K, Zhang X, Chen X, Zhong W, Du Y (2016) Constructing two-, zero- and one-dimensional integrated nanostructures: an effective strategy for high microwave absorption performance. ACS Appl Mater Interfaces 8(46):31878–31886

[9] Zhang Y, Quan B, Liu W, Liang X, Ji G, Du Y (2017) A facile one-pot strategy for fabrication of carbon-based microwave absorbers: effects on annealing and paraffin content. Dalton Trans 46(28):9097–9102

[10] Li N, Huang G, Li Y, Xiao H, Feng Q, Hu N, Fu S (2017) Enhanced microwave absorption performance of coated carbon nanotubes by optimizing the Fe_3O_4 nanocoating structure. ACS Appl Mater Interfaces 9(3):2973–2983

[11] Chen Y, Zhang A, Ding L, Liu Y, Lu H (2017) A three-dimensional absorber hybrid with polar oxygen functional groups of MWNTs/graphene with enhanced microwave absorbing properties. Compos B 108:386–392

[12] Huang T, He M, Zhou Y, Pan W, Li S, Ding B, Huang S, Tong Y (2017) Fabrication and microwave absorption of multiwalled carbon nanotubes anchored with CoS nanoplates. J Mater Sci Mater Electron 28(11):7622–7632

[13] Cao M, Qin R, Qiu C, Zhu J (2003) Matching design and mismatching analysis towards radar absorbing coatings based on conducting plate. Mater Des 24(5):391–396

[14] Lin L, Xing H, Shu R, Wang L, Ji X, Tan D, Gan Y (2015) Preparation and microwave absorption properties of multi-walled carbon nanotubes decorated with Ni-doped SnO_2 nanocrystals. RSC Adv 5(115):94539–94550

[15] Wu N, Lv H, Liu J, Liu Y, Wang S, Liu W (2016) Improved electromagnetic wave absorption of Co nanoparticles decorated carbon nanotubes derived from synergistic magnetic and dielectric losses. Phys Chem Chem Phys 18(46):31542–31550

[16] Zhang H, Hong M, Chen P, Xie A, Shen Y (2016) 3D and ternary rGO/MCNTs/Fe_3O_4 composite hydrogels: synthesis, characterization and their electromagnetic wave absorption properties. J Alloys Compd 665:381–387

[17] Zhong B, Cheng Y, Wang M, Bai Y, Huang X, Yu Y, Wang H, Wen G (2018) Three dimensional hexagonal boron nitride nanosheet/carbon nanotube composites with light weight and enhanced microwave absorption performance. Compos A 112:515–524

[18] Hu C, Liu H, Zhang Y, Zhang M, Zhang X (2019) Tuning microwave absorption properties of multi-walled carbon nanotubes by surface functional groups. J Mater Sci 54(3):2417–2426. https://doi.org/10.1007/s10853-018-2895-y

[19] Wang M, Wang H, An L, Zhang B, Huang X, Wen G, Zhong B, Yu Y (2020) Facile fabrication of Hildewintera-colademonis-like hexagonal boron nitride/carbon nanotube composite having light weight and enhanced microwave absorption. J Colloid Interface Sci 564:454–466

[20] Mustaffa M, Azis R, Abdullah N, Ismail I, Ibrahim I (2019) An investigation of microstructural, magnetic and microwave absorption properties of multi-walled carbon nanotubes/$Ni_{0.5}Zn_{0.5}Fe_2O_4$. Sci Rep 9(1):15523

[21] Syazwan M, Hashim M, Azis R, Ismail I, Kanagesan S, Hapishah A (2017) Enhancing absorption properties of Mg–Ti substituted barium hexaferrite nanocomposite through the addition of MWCNT. J Mater Sci Mater Electron 28:8429–8436

[22] Zhang K, Gao X, Zhang Q, Li T, Chen H, Chen X (2017) Preparation and microwave absorption properties of asphalt carbon coated reduced graphene oxide/magnetic $CoFe_2O_4$ hollow particles modified multi-wall carbon nanotube composites. J Alloys Compd 723:912–921

[23] Zhang B, Wang P, Xu J, Han Y, Jin D, Peng X, Hong B, Li J, Gong J, Ge H, Zhu Z, Wang X (2015) Microwave absorption and magnetic properties of cobalt ferrites/carbon nanotubes nanocomposites. NANO 10(5):1550070

[24] Yao Z, Fan X, He B, Zhang W, Bello I, Lee S, Meng X (2008) Study of in-plane orientation of epitaxial AlN films grown on (111) SrTiO. Appl Phys Lett 92(24):241911–241913

[25] Ognjanovic S, Winterer M (2018) Optimizing particle characteristics of nanocrystalline aluminum nitride. Powder Technol 326:488–497

[26] Teng C, Ma C, Chiou K, Lee T (2012) Synergetic effect of thermal conductive properties of epoxy composites containing functionalized multi-walled carbon nanotubes and aluminum nitride. Compos B 43(2):265–271

[27] Song C, Yin X, Han M, Li X, Hou Z, Zhang L, Cheng L (2017) Three-dimensional reduced graphene oxide foam modified with ZnO nanowires for enhanced microwave absorption properties. Carbon 116:50–58

[28] Liu X, Ou Z, Geng D, Han Z, Xie Z, Zhang Z (2009) Enhanced natural resonance and attenuation properties in superparamagnetic graphite-coated $FeNi_3$ nanocapsules. J Phys D: Appl Phys 42(15):155004

[29] Yang F, Jin L, Sun L, Ren X, Duan X, Cheng H, Xu Y, Zhang X, Lai Z, Chen W, Dong H, Hu W (2018) Free-standing 2D hexagonal aluminum nitride dielectric crystals for high-performance organic field-effect transistors. Adv Mater 30(34):1801891

[30] Prabhu Y, Sreedhar B, Pal U (2019) Achieving enhanced photocatalytic activity of ZnO supported on MWCNTs towards degradation of pollutants under visible light. Mater Today 8(1):419–426

[31] Zhang H, Lin G, Zhou Z, Dong X, Chen T (2002) Raman spectra of MWCNTs and MWCNT-based H_2-adsorbing system. Carbon 40(13):2429–2436

[32] Jung H, Gong Z, Liu X, Guo X, Zou C, Tang H (2019) Stokes and anti-Stokes Raman scatterings from frequency comb lines in poly-crystalline aluminum nitride microring resonators. Opt Express 27(16):22246–22253

[33] Rao G, Lu C, Su F (2007) Sorption of divalent metal ions from aqueous solution by carbon nanotubes: a review. Sep Purif Technol 58(1):224–231

[34] Qian R, Yu J, Xie L, Li Y, Jiang P (2013) Efficient thermal properties enhancement to hyperbranched aromatic polyamide grafted aluminum nitride in epoxy composites. Polym Adv Technol 24(3):348–356

[35] Vukovi G, Marinkovi A, Colic M, Ristic M, Aleksandra R, Pericgrujic A, Uskokovic P (2010) Removal of cadmium from aqueous solutions by oxidized and ethylenediamine-functionalized multi-walled carbon nanotubes. Chem Eng J 157(1):238–248

[36] He S, Wang G, Lu C, Liu J, Wen B, Liu H, Guo L, Cao M (2013) Enhanced wave absorption of nanocomposites based on the synthesized complex symmetrical CuS nanostructure and poly(vinylidene fluoride). J Mater Chem A 1(15):4685–4692

[37] Zong M, Huang Y, Zhao Y, Sun X, Qu C, Luo D, Zheng J (2013) Facile preparation, high microwave absorption and microwave absorbing mechanism of RGO–Fe_3O_4 composites. Rsc Adv 3(45):23638

[38] Zhang Y, Wang X, Cao M (2018) Confinedly implanted $NiFe_2O_4$-rGO: Cluster tailoring and highly tunable electromagnetic properties for selective-frequency microwave absorption. Nano Res 11:1426–1436

[39] Wang X, Ma T, Shu J, Cao M (2018) Confinedly tailoring Fe_3O_4 clusters-NG to tune electromagnetic parameters and microwave absorption with broadened bandwidth. Chem Eng J 332:321–330

[40] Naito Y, Suetake K (1970) Application of ferrite to electromagnetic wave absorber and its characteristics. Int Micro Symp 19(1):273–278

[41] Meng F, Wei W, Chen X, Xu X, Jiang M, Jun L, Wang Y, Zhou Z (2015) Design of porous C@Fe_3O_4 hybrid nanotubes toward their excellent microwave absorption. Phys Chem Chem Phys 18(4):2510–2516

[42] Quan B, Xu G, Li D, Liu W, Ji G, Du Y (2017) Incorporation of dielectric constituents to construct ternary heterojunction structures for high-efficiency electromagnetic response. J Colloid Interface Sci 498:161–169

[43] Li Z, Li X, Zong Y, Tan G, Sun Y, Lan Y, He M, Ren Z, Zheng X (2017) Solvothermal synthesis of nitrogen-doped graphene decorated by superparamagnetic Fe_3O_4 nanoparticles and their applications as enhanced synergistic microwave absorbers. Carbon 115:493–502